ACS APPLIED MATERIALS & INTERFACES

LETTER

www.acsami.org

Nanoporous PdNi Alloy Nanowires As Highly Active Catalysts for the Electro-Oxidation of Formic Acid

Chunyu Du,*,† Meng Chen,‡ Wengang Wang,‡ and Geping Yin†

†School of Chemical Engineering and Technology, Harbin Institute of Technology, Harbin 150001, China

‡College of Materials Science and Chemical Engineering, Harbin Engineering University, Harbin 150080, China

Supporting Information

ABSTRACT: Highly active and durable catalysts for formic acid oxidation are crucial to the development of direct formic acid fuel cell. In this letter, we report the synthesis, characterization, and electrochemical testing of nanoporous $Pd_{57}Ni_{43}$ alloy nanowires for use as the electrocatalyst towards formic acid oxidation (FAO). These nanowires are prepared by chemically dealloying of Ni from Ni-rich PdNi alloy nanowires, and have high surface area. X-ray diffraction data show that the $Pd_{57}Ni_{43}$ nanowires have the face-centered cubic crystalline structure of pure Pd, whereas X-ray photoelectron spectroscopy confirm the modification of electronic structure of Pd by electron transfer from Ni to Pd. Electrocatalytic activity of the nanowires towards FAO exceeds that of the state-of-the-art Pd/C. More importantly, the nanowires are highly resistant to deactivation. It is proposed that the high active surface area and modulated surface properties by Ni are responsible for the improvement of activity and durability. Dealloyed nanoporous $Pd_{57}Ni_{43}$ alloy nanowires are thus proposed as a promising catalyst towards FAO.

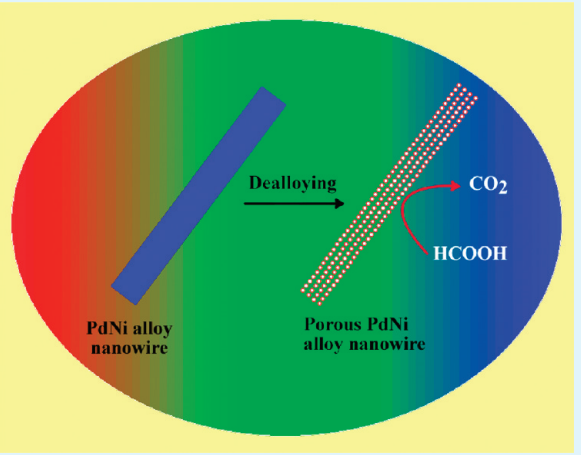

KEYWORDS: electrocatalyst, nanowires, formic acid oxidation, palladium−nickel alloy, dealloying

INTRODUCTION

Direct formic acid fuel cell (DFAFC) systems have recently been attracting great attention as promising alternative portable power sources, due to the advantages of high electromotive force, low fuel crossover, high power densities, etc.[1] However, the low active and durable catalysts for the reaction of formic acid oxidation (FAO) severely defer the development of DFAFC.[2,3] Initially, carbon supported platinum (Pt/C) was used as the FAO catalyst, but the oxidation rate was quite low because platinum was easy to be poisoned by the CO intermediates during the FAO.[4] Later, it was reported that carbon supported palladium (Pd/C) exhibited much better activity than Pt/C, but the activity was still not satisfactory, and more importantly the durability of Pd/C catalyst was in urgent need for further improvement because this catalyst deactivated quickly.[5] Hence, it is highly significant to develop new types of durable catalysts with high activity for the reaction of FAO.[6]

Nanoporous metallic structures have been explored for possible applications in electrocatalysis,[7,8] because they usually possess high surface areas, unique chemical properties, and interconnected structures that do not require any support so that the corrosion and detachment problems common for carbon supported catalysts can be avoided. Several methods have been developed to fabricate porous metallic nanostructures, such as liquid crystal template synthesis,[9] hydrothermal growth,[10] and chemical/electrochemical dealloying.[11,12] Among them, dealloying has been demonstrated to be a simple and effective way for fabricating well-defined nanoporous metallic structures.[11,12] Generally, dealloying refers to chemically/electrochemically selective dissolution of the less noble metal component(s) from an alloy, thus resulting in the formation of a porous skeleton of the more noble metal component(s).[13,14] By dealloying the Co-rich PtCo alloy, Liu and co-workers[15] synthesized nanoporous PtCo alloy catalysts that were found to exhibit distinctly enhanced catalytic activity toward methanol oxidation. Xu et al.[16] prepared PtCu bimetallic porous nanostructures through a galvanic replacement reaction using dealloyed nanoporous copper as both template and reducing agent. The resulting PtCu nanostructure showed significantly better activity toward oxygen reduction reaction than that of the commercial Pt/C catalyst. Herein, to develop more active and durable catalysts for the reaction of FAO, we report the formation, physical characterization, and electrochemical activity of nanoporous PdNi

Received: August 29, 2010
Accepted: December 20, 2010
Published: December 30, 2010

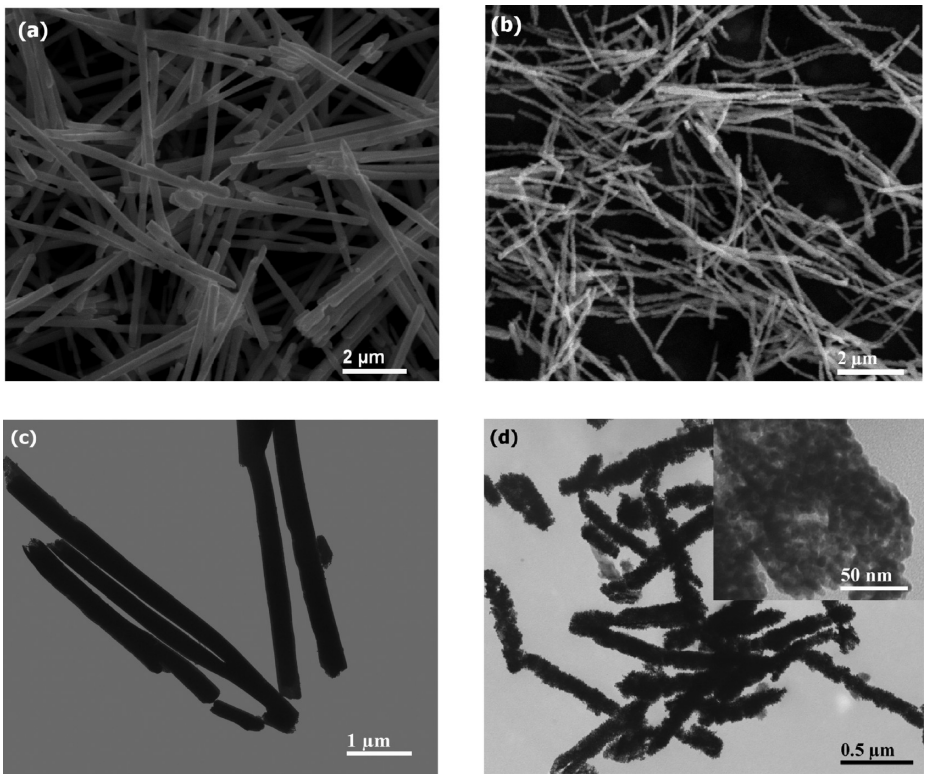

Figure 1. SEM images of (a) the Ni-rich $Pd_{25}Ni_{75}$ and (b) the nanoporous $Pd_{57}Ni_{43}$ alloy nanowires; TEM images of (c) the Ni-rich $Pd_{25}Ni_{75}$ and (d) the nanoporous $Pd_{57}Ni_{43}$ alloy nanowires.

alloy nanowires by dealloying Ni-rich PdNi nanowires that are electrodeposited in porous anodic aluminum oxide (AAO) membrane. To the best of our knowledge, this is the first time that porous Pd-based alloy nanowires are proposed as a catalyst for the reaction of formic acid oxidation.

EXPERIMENTAL SECTION

Nanoporous PdNi alloy nanowires were synthesized by electrodepositing Ni-rich PdNi alloy nanowires into the pores of AAO membrane (Whatman, Anodisc25), followed by a dealloying treatment in a mild acidic medium. The electrodeposition was conducted in a standard three-electrode electrochemical cell at a constant potential of −0.32 V (vs. RHE) on a CHI604D Potentiostat (CH Instruments Inc.). Before deposition, a layer of Cu (1−2 um) was sputtered on one side of the AAO membrane. Afterwards, the Cu-coated AAO membrane, a platinum foil and an Hg/Hg_2SO_4 electrode were used as the working, counter, and reference electrodes, respectively. The electrolyte solution consisted of 0.5 mM $Pd(NH_3)_2Cl_2$, 50 mM $NiSO_4$, and 0.1 M NH_4Cl. After deposition, the AAO membrane was removed by immersing in 2 M NaOH for more than 2 h, and the remaining PdNi alloy nanowires were filtered and washed thoroughly with deionized water and ethanol. The dealloying treatment was performed by immersing the PdNi alloy nanowires into 10 wt % H_3PO_4 solution at 50 °C for 5 h. The sample was then filtered and washed with deionized water and ethanol several times to obtain the nanoporous PdNi alloy nanowires.

The morphology of the catalysts was characterized by SEM (JEM 100CX-II) and TEM (Hitachi-7650), respectively. The composition of the catalysts was determined using the energy-dispersive X-ray spectroscopy (EDX). XRD measurements of the catalysts were performed on a Rigaku Model D/max-rB diffraction system. XPS characterization was carried out with a Physical Electronics PHI 5600 multitechnique system.

Electrochemical measurements were conducted using a CHI604D Potentiostat in a three-electrode electrochemical cell at room temperature. A glass carbon electrode, on which the catalysts were covered with the Pd loading of 3 μg, was used as the working electrode. A Pt foil and an Hg/Hg_2SO_4 electrode were used as the counter and reference electrodes, respectively. All the electrode potentials quoted in this paper are converted to the reversible hydrogen electrode (RHE) scale by adding 0.68 V to the measured potential. The hydrogen adsorption−desorption experiment was carried out in a 1 M H_2SO_4 solution at a scan rate of 50 mV s^{-1}. The catalytic activity of the catalysts toward the reaction of FAO was evaluated by CV and chronoamperometry (CA) tests in a 0.5 M H_2SO_4 + 0.5 M HCOOH solution. Prior to electrochemical measurements, the electrolytes were deoxygenated by bubbling with high-purity N_2 for 30 min.

RESULTS AND DISCUSSION

Images a and b in Figure 1show typical scanning electron microscopy (SEM) images of the PdNi alloy nanowires before and after the dealloying treatment. Before dealloying, the PdNi alloy nanowires (Figure 1a) had a smooth surface and average diameter of ∼250 nm, consistent with the pore diameter of the AAO membrane used. Energy-dispersion X-ray spectroscopy (EDX) characterization revealed that the composition of these nanowires was a Ni-rich $Pd_{25}Ni_{75}$. After dealloying, however, the PdNi alloy nanowires (Figure 1b) became roughened, with the average diameter shrank to ∼150 nm. Moreover, the composition of the nanowires was changed to Ni-poor $Pd_{57}Ni_{43}$. These

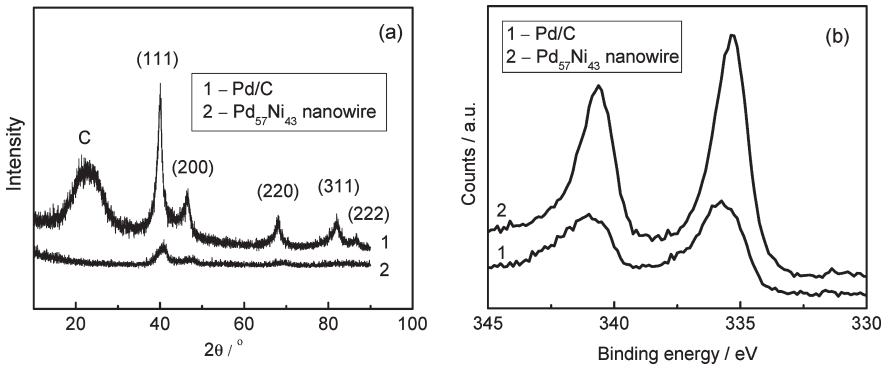

Figure 2. (a) XRD patterns and (b) Pd 3d XPS spectra of the Pd/C and the nanoporous $Pd_{57}Ni_{43}$ alloy nanowires.

changes were attributed to the chemically selective dissolution of Ni, leading to nanoporous PdNi alloy nanowires with Pd-enriched composition. Figure 1c and d present transmission electron microscopy (TEM) images of the PdNi alloy nanowires before and after the dealloying treatment. Apparently, the starting $Pd_{25}Ni_{75}$ nanowires (Figure 1c) were continuous and dense, and uniform in diameter along the entire wires. Their average diameter was ~250 nm, in accordance with the SEM observation. After dealloying, the resulting $Pd_{57}Ni_{43}$ nanowires (Figure 1d) turned to be highly rough, and their diameter was much smaller than that of the $Pd_{25}Ni_{75}$ nanowires. From the inset in Figure 1d, a large density of nanopores with size of 3−6 nm were distributed along the $Pd_{57}Ni_{43}$ nanowires, forming high active surface area.

Crystalline structure of the nanoporous $Pd_{57}Ni_{43}$ alloy nanowires and the conventional Pd/C were characterized and Figure 2a gives their XRD patterns. For the Pd/C, the five peaks located at 2θ values of ca. 40, 47, 68, 83, and 86° corresponded to the characteristic (111), (200), (220), (311), and (222) planes of pure Pd, respectively, indicating that the Pd/C catalyst was with face-centered cubic (fcc) crystalline structure. For the nanoporous $Pd_{57}Ni_{43}$ nanowires, only diffraction peaks corresponding to (111), (200), and (220) characteristic planes of Pd were clearly observed, and no diffraction peaks from either pure Ni or Ni-rich fcc phase were detected, indicating that Ni might enter into the Pd lattice forming the PdNi solid solution. Also, it was found that the diffraction peaks of $Pd_{57}Ni_{43}$ nanowires shifted to high-angle values from the original peaks of Pd, suggesting that the lattice parameters of $Pd_{57}Ni_{43}$ nanowires were decreased by addition of Ni, which might be good for the catalytic activity toward FAO.

XPS was employed to analyze surface composition and the electronic state of the porous $Pd_{57}Ni_{43}$ alloy nanowires. It was found that the Pd/Ni atomic ratio on the surface of $Pd_{57}Ni_{43}$ nanowires was 4.4, which was higher than the bulk composition, indicating that the nanoporous PdNi alloy nanowires had a Pd-enriched outer surface, consistent with the selective dissolution of Ni. The Pd 3d XPS spectra of the Pd/C and $Pd_{57}Ni_{43}$ nanowires are shown in Figure 2b. Apparently, both the spectra displayed a doublet that consisted of a high-energy peak ($Pd3d_{3/2}$) and a low-energy peak ($Pd3d_{5/2}$). For the conventional Pd/C, the $Pd3d_{5/2}$ peak was located at ~335.7 eV, indicating that the surface was highly oxidized. For the porous $Pd_{57}Ni_{43}$ alloy nanowires, however, the $Pd3d_{5/2}$ peak was located at ~335.3 eV, which was a negative shift of ~0.2 eV from 335.5 eV for the pure metallic Pd,[17] suggesting that the surface consisted mainly of metallic state Pd. This shift of binding energy resulted from the modification of electronic structure of palladium by slight electron transfer from Ni to Pd, consistent with the electronegativity of Pd and Ni. It was believed that this electron transfer contributed to the enhanced oxidation of CO intermediate, that is, to the improved CO tolerance,[18] which might be good for the formic acid oxidation.

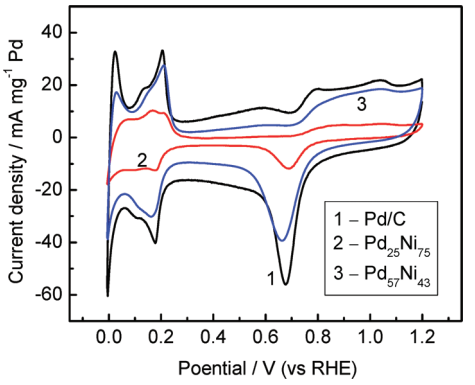

Figure 3. Cyclic voltammograms of the Pd/C, the $Pd_{25}Ni_{75}$, and nanoporous $Pd_{57}Ni_{43}$ alloy nanowires in 1 M H_2SO_4 at a scan rate of 50 mV s^{-1} under a N_2 atmosphere.

Electrochemical behavior of the nanoporous $Pd_{57}Ni_{43}$ alloy nanowires was characterized by cyclic votammetry (CV). Figure 3 shows CV curves of the Pd/C, the original $Pd_{25}Ni_{75}$ and nanoporous $Pd_{57}Ni_{43}$ alloy nanowires in 1 M H_2SO_4 solution at a scan rate of 50 mV s^{-1}. The peaks below 0.3 V were attributed to the hydrogen adsorption and desorption processes, while those above 0.5 V were assigned to the oxidation of surface metal and the reduction of thus formed oxides. The peaks for the $Pd_{25}Ni_{75}$ nanowires were significantly lower than those for the Pd/C, suggesting the small surface area of the nanowires before dealloying. After dealloying treatment, however, current peaks for the porous $Pd_{57}Ni_{43}$ alloy nanowires were remarkably enhanced and comparable to those of the Pd/C, suggesting that their surface area was greatly increased by forming the nanoporous structure, which was in accordance with the TEM results. The quantity of the electric charge for the reduction of metal oxides formed over the top layer of the metals was employed to evaluate the specific active surface area of the Pd and PdNi alloy nanowires.[19] The calculated values were 54.7, 15.1, and 58.4 mC mg^{-1} Pd for the Pd/C, the $Pd_{25}Ni_{75}$ and $Pd_{57}Ni_{43}$ alloy nanowires, respectively, indicating that the $Pd_{57}Ni_{43}$ alloy nanowires had higher specific active surface area than the Pd/C.

We evaluated the catalytic activity and durability of the porous $Pd_{57}Ni_{43}$ alloy nanowires towards the reaction of FAO. Because the Pd/C catalyst has much promising activity towards the FAO

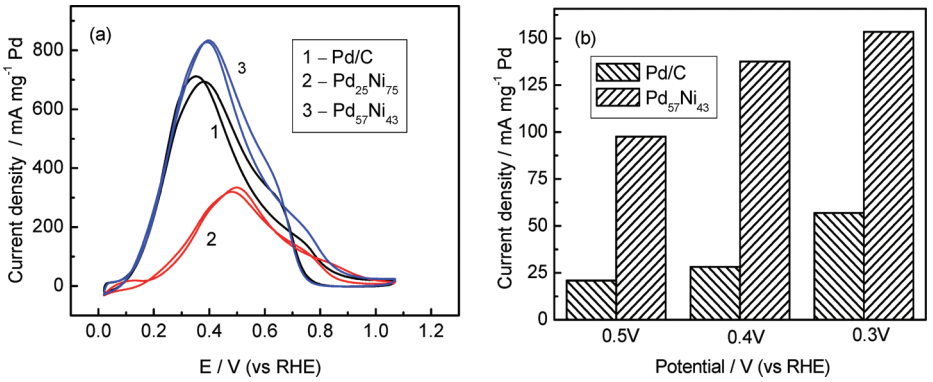

Figure 4. (a) Cyclic voltammograms of the Pd/C, the $Pd_{25}Ni_{75}$ and nanoporous $Pd_{57}Ni_{43}$ alloy nanowires in a solution of 0.5 M HCOOH and 0.5 M H_2SO_4 at a scan rate of 50 mV s^{-1}, (b) Polarization current density of the Pd/C and nanoporous $Pd_{57}Ni_{43}$ alloy nanowires in 0.5 M HCOOH and 0.5 M H_2SO_4 solution at different potentials for 15 min.

reaction, it is meaningful to assess the catalytic activity of $Pd_{57}Ni_{43}$ nanowires by comparing with that of Pd/C. Figure 4a displays the CV profiles of the Pd/C, the $Pd_{25}Ni_{75}$, and porous $Pd_{57}Ni_{43}$ alloy nanowires in a solution of 0.5 M HCOOH and 0.5 M H_2SO_4. A large current peak at 0.2−0.6 V and an indistinct shoulder at 0.6−0.8 V were observed, which corresponded to the reaction of FAO via the direct pathway and the CO pathway, respectively.[20] Apparently, the FAO on the Pd/C and PdNi alloy nanowires was mainly through the direct pathway, in agreement with the previous report.[21] It could be seen that the nanoporous $Pd_{57}Ni_{43}$ nanowires showed an activity 20% higher than that of the Pd/C, although the original $Pd_{25}Ni_{75}$ alloy nanowires had rather low activity as a result of the small active surface area. This improvement might be attributed to two aspects: (1) the dealloying process remarkably increased the active surface area of the nanowires, offering more active sites necessary for the formic acid dissociation; (2) more importantly, the modification of electronic structure of palladium by Ni facilitated the removal of poisoning intermediates on Pd, preventing the accumulation of poisoning intermediates. Figure 4b gives the steady-state current density of the Pd/C and porous $Pd_{57}Ni_{43}$ alloy nanowires in 0.5 M HCOOH+0.5 M H_2SO_4 solution polarized at different potentials for 15 min. The current density on the nanoporous $Pd_{57}Ni_{43}$ alloy nanowires was several times higher than that on the Pd/C. Consistently, as revealed by the detailed chronoamperometric data in the Supporting Information, the current transients presented weaker poisoning effect on the $Pd_{57}Ni_{43}$ nanowires than on the Pd/C. This exciting result clearly demonstrated that the nanoporous $Pd_{57}Ni_{43}$ alloy nanowires were much more durable for the reaction of FAO than the Pd/C, especially at high overpotential region where FAO follows the CO pathway and the CO poisoning is more significant, verifying that the presence of Ni was helpful in preventing the accumulation of poisoning intermediates.

CONCLUSIONS

In summary, in this letter, we synthesize nanoporous $Pd_{57}Ni_{43}$ alloy nanowires by chemically dealloying the electrodeposited $Pd_{25}Ni_{75}$ nanowires. The $Pd_{57}Ni_{43}$ nanowires have the crystalline structure of pure Pd, and show well-defined porous features with a pore size of 3−6 nm. The porous nanowires exhibit enhanced catalytic activity toward formic acid oxidation, and more importantly, they are highly resistant to deactivation. It is revealed that the modulation of Ni on the electronic structure of palladium as well as the high surface area is mainly responsible for the activity and durability improvement. In addition, the nanoporous $Pd_{57}Ni_{43}$ alloy nanowires are well interconnected and do not require any support so that the corrosion and detachment problems that nanoparticle/support systems often suffer can be avoided. Thus, the nanoporous $Pd_{57}Ni_{43}$ nanowires show substantial promise as an efficient anode catalyst for direct formic acid fuel cells.

ASSOCIATED CONTENT

Supporting Information. Synthesis details and TEM characterization of the Pd/C catalyst (PDF). This material is available free of charge via the Internet at http://pubs.acs.org.

AUTHOR INFORMATION

Corresponding Author

*E-mail: cydu@hit.edu.cn. Tel: +86-451-86403216. Fax: +86-451-86413720.

ACKNOWLEDGMENT

This work was supported by the Harbin Talents Foundation in the Innovation of Science and Technology under Contact 2008RFQXG059, the Natural Scientific Research Innovation Foundation in Harbin Institute of Technology, and the National Science Foundation of China under Contract 20706010 and 20876029.

REFERENCES

(1) Yu, X.W.; Pickup, P.G. *J. Power Sources* **2008,** *182,* 124–132.
(2) Waszczuk, P.; Barnard, T.M.; Rice, C.; Masel, R.I.; Wieckowsk, A. *Electrochem. Commun.* **2002,** *4,* 599–603.
(3) Seland, F.; Tunold, R.; Harrington, D.A. *Electrochim. Acta* **2008,** *53,* 6851–6864.
(4) Rice, C.; Ha, S.; Masel, R.I.; Waszczuk, P.; Wieckowski, A.; Barnard, T. *J. Power Sources* **2002,** *111,* 83–89.
(5) Zhu, Y.M.; Khan, Z.; Masel, R.I. *J. Power Sources* **2005,** *139,* 15–20.
(6) Wang, J.J.; Chen, Y.G.; Liu, H.; Li, R.Y.; Sun, X.L. *Electrochem. Commun.* **2010,** *12,* 219–222.
(7) Ding, Y.; Chen, M.W.; Erlebacher, J. *J. Am. Chem. Soc.* **2004,** *126,* 6876–6877.
(8) Ji, C.X.; Searson, P.C. *Appl. Phys. Lett.* **2002,** *81,* 4437–4439.
(9) Yamauchi, Y.; Sugiyama, A.; Morimoto, R.; Takai, A.; Kuroda, K. *Angew. Chem., Int. Ed.* **2008,** *47,* 5371–5373.

(10) Koczkur, K.; Yi, Q.F.; Chen, A.C. *Adv. Mater.* **2007,** *19*, 2648–2652.
(11) Yu, J.S.; Ding, Y.; Xu, C.X.; Inoue, A.; Sakurai, T.; Chen, M.W. *Chem. Mater.* **2008,** *20*, 4548–4550.
(12) Liu, H.T.; He, P.; Li, Z.Y.; Li, J.H. *Nanotechnology* **2006,** *17*, 2167–2173.
(13) Erlebacher, J.; Aziz, M.J.; Karma, A.; Dimitrov, N.; Sieradzki, K. *Nature* **2001,** *410*, 450–453.
(14) Erlebacher, J.; Sieradzki, K. *Scr. Mater.* **2003,** *49*, 991–996.
(15) Liu, L.F.; Pippel, E.; Scholz, R.; Gősele, U. *Nano Lett.* **2009,** *9*, 4352–4358.
(16) Xu, C.X.; Zhang, Y.; Wang, L.Q.; Xu, L.Q.; Bian, X.F.; Ma, H.Y.; Ding, Y. *Chem. Mater.* **2009,** *21*, 3110–3116.
(17) Adams, B.; Ostrom, C.; Chen, A. *Langmuir* **2010,** *26*, 7632–7637.
(18) Park, K.W.; Choi, J.H.; Kwon, B.K.; Lee, S.A.; Sung, Y.E.; Ha, H. Y.; Hong, S.A.; Kim, H.H.; Wieckowski, A. *J. Phys. Chem. B* **2002,** *106*, 1869–1877.
(19) Baldauf, M.; Kolb, D.M. *J. Phys. Chem.* **1996,** *100*, 11375–11381.
(20) Wang, R.F.; Liao, S.J.; Ji, S. *J. Power Sources* **2008,** *180*, 205–208.
(21) Ha, S.; Larsen, R.; Zhu, Y.; Masel, R.I. *Fuel Cells* **2004,** *4*, 337–343.